THE BALTIC JOURNAL
OF ROAD AND BRIDGE ENGINEERING

2012
7(3): 212–219

EFFECT OF SLAB CURLING ON BACKCALCULATED MATERIAL PROPERTIES OF JOINTED CONCRETE PAVEMENTS

Tae-Seok Yoo[1], Jin-Sun Lim[2], Jin-Hoon Jeong[3] ✉

[1]*Expressway and Transportation Research Institute, Korea Expressway Corporation, 50-5, Sancheok-ri, Dongtan-myeon, Hwaseong-si, Gyeonggi-do 445-812, Korea*
[2, 3]*Dept of Civil Engineering, Inha University 253, Yonghyeon-dong, Nam-gu, Incheon 402-751, Korea*
E-mails: [1]*taeseok@ex.co.kr;* [2]*coreplay@hanmail.net;* [3]*jhj@inha.ac.kr*

Abstract. Different backcalculation algorithms produce different elastic moduli which are used as a key indicator of structural capacity of concrete pavements. Accordingly, the elastic moduli backcalculated by various backcalculation algorithms have been evaluated using the elastic moduli of cores of concrete pavement layers measured in the laboratory. However, variation in the backcalculated elastic modulus, even within a pavement section, is a significant issue in the concrete pavement evaluation. In the present work, deflections of jointed concrete pavement under a Falling Weight Deflectometer (FWD) loading were measured for 48 h at the KEC (Korea Expressway Corporation) test road. The curling effect on the backcalculated elastic modulus of the concrete slab was investigated using the different temperature gradients and slab curl conditions arising at different measurement times. The elastic moduli of the concrete pavement layers were backcalculated using the measured deflection basins, the AREA method and the method of equivalent thickness (MET). A basic concept to adjust the cyclic variation in the backcalculated elastic modulus due to the slab curling using the temperature difference between the top and bottom of the slab is presented. Measured data of deflection and load transfer efficiency (LTE) of the tested joints verify the curling effect on the backcalculated structural capacity of the concrete pavements.

Keywords: concrete pavement, backcalculation, elastic modulus, deflection, Falling Weight Deflectometer (FWD), load transfer efficiency (LTE).

1. Introduction

The temperature of concrete pavement continuously changes because of variation in the ambient temperature. A concrete slab curls because of variation in the amount of expansion or contraction between the top and bottom of the slab due to an uneven vertical temperature distribution. Downward curling shown in Fig. 1a indicates a downward displacement of the slab corner caused by expansion of the slab top due to a higher concrete temperature than at the bottom. Conversely, upward curling shown in Fig. 1b is an upward displacement of the slab corner due to lower concrete temperature at the slab top. The daily cycles of upward and downward curling are repeated over the lifetime of concrete pavement, because the ambient temperature continuously passes through a daily cycle.

The deflection of a concrete slab under a Falling Weight Deflectometer (FWD) loading has been used in backcalculation of the elastic modulus of pavement layers. The backcalculated elastic modulus has been used as a key criterion in assessing the in situ structural capacity of pavement. Additionally, the joint's load transfer efficiency (LTE) is useful in the assessment of the structural capacity of the joint. Optimal maintenance and rehabilitation strategies for concrete pavements also make use of FWD test results. Accordingly, there have been efforts to enhance the accuracy of the measured responses and backcalculated elastic moduli of concrete pavement layers (Karadelis 2008; Li, White 2000; Lin *et al.* 1998). However, variation in the backcalculated elastic modulus caused by change in configuration of the concrete pavement due to slab curling has not been successfully addressed because the effect of slab curling is not taken into consideration in any existing backcalculation algorithms.

The FWD deflections of concrete pavement sections at the KEC (Korea Expressway Corporation) test road were measured over a 48 h period in order to investigate the effect of curling on the backcalculated structural capacity of the pavement which is often represented by the elastic modulus of the slab. A basic concept to adjust the cyclic variation in the backcalculated elastic modulus due

ISSN 1822-427X print / ISSN 1822-4288 online
doi:10.3846/bjrbe.2012.29
http://www.bjrbe.vgtu.lt

to slab curling was studied using the relationship between the backcalculated elastic modulus and the temperature difference between the top and bottom of the concrete slab. Additional data was also collected at the joints in order to verify the effect of slab curling on the backcalculated structural capacity of the concrete pavements.

2. Field test program

The KEC test road includes 2 lanes of 22 jointed plain concrete pavement (JPCP) sections having variables of slab thickness (250, 300 and 350 mm), subbase materials (lean concrete, aggregates and asphalt), and subbase thickness (120, 150 and 180 mm) (Jeong 2008). Among the 22 JPCP sections, a 300 m length consisting of 3 continuous sections (sections 4–0, 5–0 and 6–0) paved on the same day were selected as sample sections for this study. The JPCP sections were paved on October 4th, 2002, approximately between 8 am and 5 pm. The slab thickness of the sections is 300 mm but the sections consist of different subbase (lean concrete) layer thicknesses. The thicknesses of the subbase layers are 120, 150 and 180 mm, respectively. However, the actual thicknesses of the subbase layers of the sections obtained by measuring the lengths of the subbase cores are 117, 168 and 183 mm. The mixture proportions of the concrete slab and lean concrete subbase are shown in Table 1. The equivalent linear temperature difference (Mohamed, Hansen 1997) between the top and bottom of the slab was calculated using the temperature data collected at different depths of the slab. The sections showed different built-in temperature differences at the final setting of the concrete slab measured by *ASTM C 403: 2002 Annual Book of ASTM Standards: Standard Test Method for Time of Setting of Concrete Mixtures by Penetration Resistance.* The built-in temperature difference of section 4–0 paved in the morning was +10.7 °C while that of section 6–0 paved in the afternoon was recorded as –8.0 °C. The sections placed at different times of the day showed different long-term joint behaviours, because of the different built-in temperature (Jeong *et al.* 2006). Geographically, sections 4-0 and 5–0 are located in fill areas and section 6-0 is located at the boundary of fill and cut sections. The bearing capacities of the subgrade of the sections measured by a plate bearing test using a 300 mm diameter plate are 199, 178 and 221 kPa/mm, respectively.

A continuous section of 5 slabs in the travelling lane was randomly selected to measure deflections at slab centres and joints using the FWD, and to calculate foundation moduli, the elastic layer moduli, and LTE of the joints using the measured deflections and deflection basins. A total of 12 FWD tests were performed over a 48 h period between October 4th and October 5th, 2004, exactly 2 years after construction of the pavement. During the test, ambient temperature data was collected from a weather station installed at the test road. The temperature of

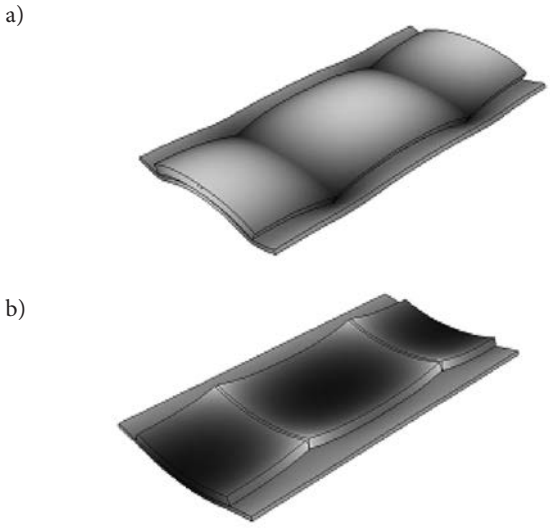

Fig 1. Curling of concrete pavement: a – downward curling; b – upward curling

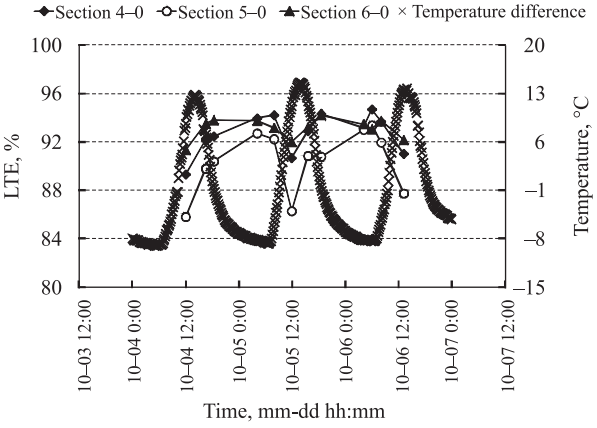

Fig. 2. Temperature data collected during test period

Table 1. Mixture proportion in 1 m^3 of concrete

Layer	W/C	S/a	W, kg	C, kg	S, kg	G, kg		AE, g	Slump, mm	Air, %
						G1 (32 mm)	G2 (19 mm)			
Concrete slab	0.423	0.377	144	340	682	660	532	510	25	4.5
Lean concrete subbase	0.759	0.331	120	158	720	735	715	–	–	–

the slab surface was also measured using a temperature sensor on the FWD. In addition, temperature profiles of the slab were obtained using temperature sensors installed during construction at different slab depths. All the temperature related data showed daily cycles, as shown in Fig. 2. Three tests were performed between 4 am to 8 am and the other 3 test times were between 12 pm and 6 pm in the course of a day. The continuously varying ambient temperatures influenced slab behaviour and curling, consequently affecting the measured deflections; FWD tests were performed using 4 levels of loading, as presented in Table 2, by changing the height of the dropped weight. The loading was applied a total of 8 times for each position by applying 4 levels of the loading two times each. However, the data produced by the load level of 40 kN (load Level 1) was not used in the analysis, because the measured deflections and calculated foundation moduli, elastic moduli, and LTE based on the loading showed peculiar trends in comparison to those analyzed with the other levels of loading. Thus, the deflections produced by the loadings from Level 2 to Level 4 were used in the study.

3. Curling effect on backcalculated elastic modulus of slab

The elastic moduli of the concrete slabs were backcalculated by analyzing the deflection data collected from the FWD tests. The AREA method and the method of equivalent thickness (MET) were used to analyze the data. The backcalculated elastic moduli showed daily variations with 24 hour-cycles, because of slab curling. The elastic moduli were calibrated on the basis of the temperature difference between the top and bottom of the slab, which causes the slab curling.

Table 2. Applied FWD loading

Level of loading	Magnitude of load, kN
1	35–40
2	53–58
3	74–77
4	111–116

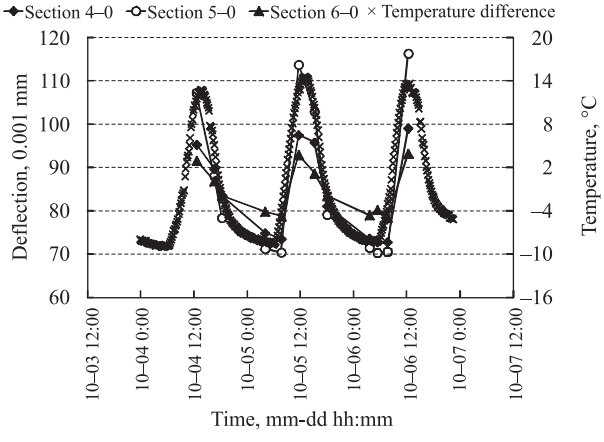

Fig. 3. Deflection of slab center measured at loading point

3.1. Deflection of slab centre due to FWD loading

As previously noted, FWD deflections at the centre of slab were measured. The variation in mean deflections of the 5 slabs with time is shown in Fig. 3. The deflections produced by the different magnitudes of loading (Level 2 to Level 4) were converted to deflections corresponding to the standard loading (Level 1, 40 kN) assuming a linear relationship between the slab deflection and the applied loading. The deflections of the slab centres showed daily cycles and the values ranged extensively between 70 and 120 mm. The variation in the deflection formed daily cycles; this is a result of the slab curling due to the continuously varying slab temperature. Larger deflections of the slab centres were observed in the afternoon, when downward slab curling existed, due to the existence of a positive temperature difference between the top and bottom of the slab. On the contrary, smaller deflections were measured in the morning, when upward slab curling developed, because of a negative temperature difference. It was estimated that the upward slab curling enhanced contact between the slab bottom and subbase at the slab centre. Accelerated changes in the deflections were observed between the period of the min and max peaks while slower changes were monitored between the period of the max and min peaks, as shown in Fig. 3. The trend of the variation in the centre slab deflections corresponded closely to the trend of the measured temperature.

The slabs in section 4–0 placed in the morning were expected to experience larger upward curling than slabs in the other sections, because of their substantially higher built-in temperature difference (Jeong *et al.* 2006). However, the slabs in section 5–0, placed near midday, showed the largest mean daily deflections, rather than those in section 4–0. The larger mean daily deflections of the slabs in section 5–0 were mainly caused by the larger max deflection peaks arising in the section 5–0 slabs than those of other sections measured. The slabs in section 5–0 showed the smallest min peaks (measured in the morning) as well. The slabs in section 6–0, placed in the afternoon, had the smallest built-in temperature difference and presented the smallest mean daily deflections, as expected. It is also noted that these slabs showed the smallest max peak in the afternoon and the largest min peak in the morning. Overall, however, because of the limited data available for the study, it was difficult to discern the effect of the built-in temperature on the deflection of the slab centre.

3.2. Elastic modulus backcalculated by AREA method

The concrete elastic moduli of the slabs were backcalculated from the FWD deflection data. The AREA method (*AASHTO: 1998 AASHTO Guide for Design of Pavement Structures*) and the method of equivalent thickness (MET) were used in the backcalculation of the elastic moduli of the pavement layers. The deflections measured using 7 sensors were used in the calculation of the deflection basin

area, which has the unit of length, as shown in Eq (1) (Ioannides 1990):

$$AREA = \frac{\Delta}{2d_0}\left[d_0 + 2(d_1 + d_2 + \cdots + d_{n-1}) + d_n\right], \quad (1)$$

where *AREA* – deflection basin area, inch; d_i – deflection measured by i^{th} sensor, mil; n – number of sensors – 1; Δ – spacing of sensors is 12 inch according to *AASHTO: 1998 AASHTO Guide for Design of Pavement Structures*.

The deflection basin area was originally used in the development of algorithms and nomographs to backcalculate resilient moduli of asphalt pavement layers (Hoffman, Thompson 1982). The deflection basin area concept has also been used in the backcalculation of the foundation modulus and elastic modulus of concrete pavements since the late 1980s (Talvik, Aavik 2009). The relationship between the deflection basin area and radius of relative stiffness was studied in order to convert the measured deflection basin to the radius of relative stiffness of the concrete slab, as given by Eq (2) (*AASHTO: 1998 AASHTO Guide for Design of Pavement Structures*) (Hall, Mohseni 1991):

$$l_k = \left[\frac{\ln\left(\frac{36 - AREA}{1812.279133}\right)}{-2.559340}\right]^{4.387009}, \quad (2)$$

where l_k – the radius of relative stiffness with the unit of length.

The radius of relative stiffness and max deflection measured at the position of the loading plate were used in the calculation of the foundation modulus derived from expressions suggested by Westergaard *et al.* (1939) as follows:

$$k = \left(\frac{P}{8d_0 l_k^2}\right)\left\{1 + \left(\frac{1}{2\pi}\right)\left[\ln\left(\frac{a}{2l_k}\right) + \gamma - 1.25\right]\left(\frac{a}{l_k}\right)^2\right\}, \quad (3)$$

where k – foundation modulus, pci; P – FWD load, lb; a – radius of loading plate, inch; γ – Euler's constant (= 0.57721566490).

The foundation moduli backcalculated by following the procedure outlined from Eq (1) to Eq (3) are composite values representing the subgrade, subbase and base layers, and the values also vary in daily cycles, as shown in Fig. 4. The slabs in section 5–0, which manifest the largest daily variations in the slab center deflection, also showed the largest daily variations in the backcalculated foundation modulus, while the slabs in section 6–0 showed the smallest daily variations among the 3 sections. The foundation moduli of the slabs in section 5–0 showed the largest max peaks in the morning, when upward curling prevailed, and the smallest min peaks in the afternoon, when downward curling was most prevalent. On the other hand, the slabs in section 6-0 showed the smallest max peaks and the largest min peaks. This implies that the value of the backcalculated foundation moduli is significantly influenced by slab curling. Again, because of the slab curling, the value of the foundation moduli of the 3 sections ranged cyclically between 32 and 70 kPa/mm.

The elastic modulus of the concrete slab was calculated using the radius of relative stiffness and the foundation modulus as follows:

$$E = \frac{12(1-\nu^2)kl_k^4}{h^3}, \quad (4)$$

where E – elastic modulus of concrete slab, psi; ν – Poisson's ratio of concrete; h – slab thickness, inch.

The elastic moduli of the concrete slabs backcalculated by the AREA method ranged between 25 and 38 GPa, making daily cycles as shown in Fig. 5. The elastic moduli at the zero temperature gradient stayed largely fell in the middle region within the range. The slab curling also led to substantial variation in the backcalculated elastic modulus, yielding a similar trend to that of the backcalculated foundation modulus. The backcalculated elastic modulus showed max peaks in the morning, when upward curling developed, and min peaks in the afternoon, when downward curling occurred. However, in contrast with the

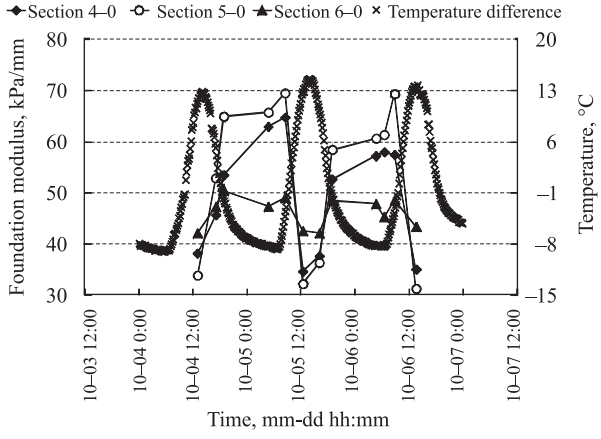

Fig. 4. Foundation modulus backcalculated by AREA method

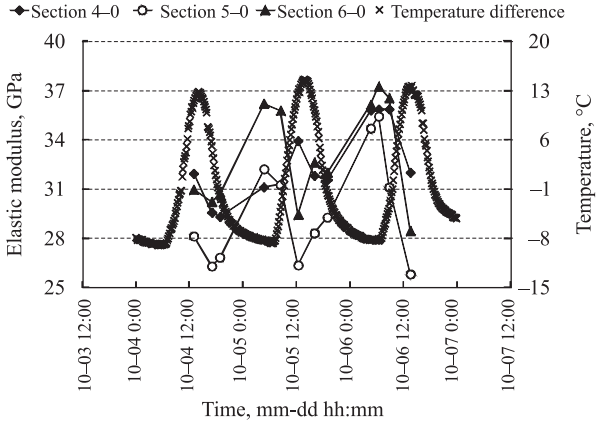

Fig. 5. Elastic modulus of concrete slab backcalculated by AREA method

foundation modulus, the slabs in section 6–0 showed the largest max peaks among the 3 sections. The section 5–0 slabs showed the smallest min peaks. However, it was difficult to determine which section showed the smallest max peaks and the largest min peaks, because the cyclic trend of the backcalculated elastic moduli of the slabs in section 4–0 was not clear, as shown in the Fig. 5.

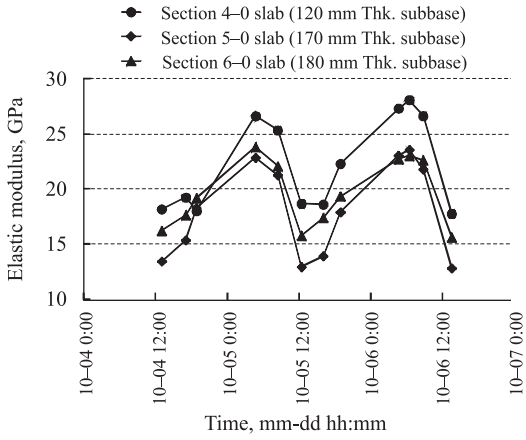

Fig. 6. Elastic modulus of concrete slab backcalculated by MET

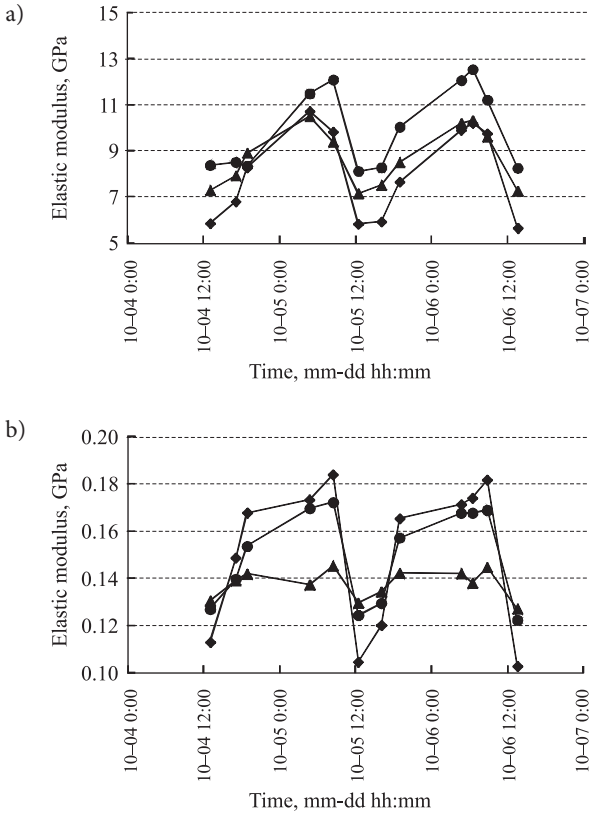

Fig. 7. Elastic modulus of subbase and subgrade backcalculated by MET: a – lean concrete subbase; b – subgrade: Section 4–0 slab (120 mm Thk. subbase); Section 5–0 slab (170 mm Thk. subbase); Section 6–0 slab (180 mm Thk. subbase)

3.3. Elastic modulus backcalculated by MET

The elastic moduli of the pavement layers were back-calculated by the method of equivalent thickness (MET). The MET transforms the pavement layers with different thicknesses, elastic moduli and Poisson's ratios to a layer with uniform material properties. The resulting equivalent thickness of the layer is calculated using the thicknesses and material properties of the pavement layers as follows (Šiaudinis 2006; Ullidtz 1987):

$$h_e = h_1 \sqrt{\frac{E_1}{E_2}\frac{(1-\nu_2^2)}{(1-\nu_1^2)}}, \quad (5)$$

where h_e – equivalent thickness, inch; h_i – thickness of layer i, inch; E_i – elastic modulus of layer i, psi; ν_i – Poisson's ratio of layer i.

In the case of Eq (5) 2 layers are transformed to a single layer with an elastic modulus of E_2 and a Poisson's ratio of ν_2. The optimal elastic moduli of the pavement layers were obtained by iteratively comparing the deflection basins calculated by a commercial program which used the MET algorithm to those measured by 7 geophones of the FWD. The basic assumption of the program, which uses multilayer elastic analysis, is that the pavement layers are bonded to each other. This is not applicable to curled concrete slabs, which are unbounded from the subbase layer. As a result, the elastic moduli of the concrete slabs backcalculated by the MET were lower than those backcalculated by the AREA method, as shown in Fig. 6.

The elastic moduli backcalculated by the MET cycled between 13 and 28 GPa. The elastic moduli at the zero temperature gradient also largely remained in the middle area within the range. The elastic moduli showed max peaks in the morning and min peaks in the afternoon, in agreement with those backcalculated by the AREA method. This indicates that the slab curling also influenced the elastic modulus backcalculated by the MET. The slabs in section 4–0 placed in the morning showed relatively larger elastic moduli and the slabs in section 5–0 showed relatively lower elastic moduli for both the concrete slab and the lean concrete subbase. In contrast with the results of the AREA method, the cyclic trend of the elastic moduli of the slabs in section 4–0 backcalculated by the MET was very clear.

Even though the values were much lower, the trend of the backcalculated elastic moduli of the lean concrete subbase was similar to that of the concrete slabs, as shown in Fig. 7a. The backcalculated elastic moduli of the subgrade shown in Fig. 7b also showed roughly the same trend as the foundation moduli backcalculated by the AREA method (Fig. 4).

3.4. Adjustment of backcalculated elastic modulus using temperature difference

The elastic moduli of 150 mm diameter cylindrical cores of the concrete slabs were measured following *ASTM C 469: 2002 Annual Book of ASTM Standards: Standard Test Method for Static Modulus of Elasticity and Poisson's Ratio*

of Concrete in Compression. Strain gauges were installed on the sides of the cores to measure the vertical deformations of the cores when compressive loadings are applied on the axes of the cores. The measured elastic modulus of the cores was 31.1 GPa and it stayed within the range of the elastic moduli backcalculated by the AREA method. However, the measured value was higher than the highest elastic modulus backcalculated by the MET. The differences between the measured and backcalculated elastic moduli showed a linear relationship with the temperature differences between the top and bottom of the concrete slab, as shown in Fig. 8. The improved correlation between the elastic modulus difference based on the MET and temperature difference shown in the figure was primarily because of the clearer trend of the elastic moduls backcalculated by the MET relative to that backcalculated by the AREA method. The backcalculated elastic moduli were adjusted using the linear relationship following Eqs (6) and (7):

$$\Delta E = a\Delta T + b, \tag{6}$$

$$E = E_{bc} + \Delta E, \tag{7}$$

where ΔE – difference between measured and backcalculated elastic modulus, GPa; ΔT – temperature different between top and bottom of concrete slab, °C; *a, b* – adjustment coefficients; E – adjusted elastic modulus, GPa; E_{bc} – backcalculated elastic modulus, GPa.

The variations in the elastic moduli of the concrete slabs backcalculated by both the AREA method and MET were successfully corrected by application of the adjustment procedure. The corrected elastic moduli are compared to the backcalculated elastic moduli prior to the adjustment, as shown in Fig. 9.

The elastic moduli backcalculated by the MET showed better convergence to the measured elastic modulus than those backcalculated by the AREA method, because of the

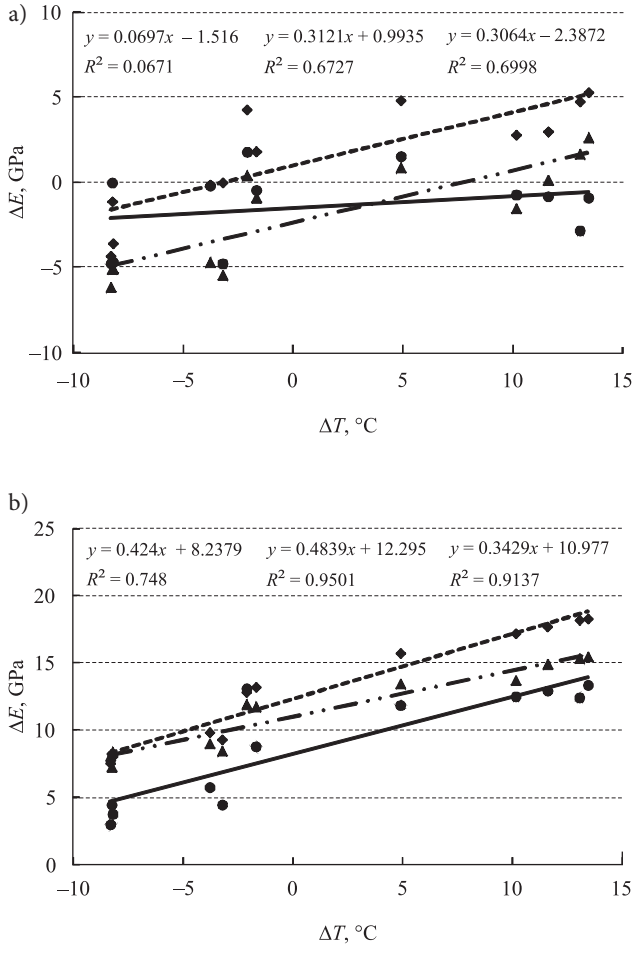

Fig. 8. Linear relationship of difference between measured and backcalculated elastic modulus with temperature difference: a – AREA method; b – MET: ● Section 4–0; ◆ Section 5–0; ▲ Section 6–0; ——— Regression_4–0; – – – Regression_5–0; . . – . . Regression_6–0

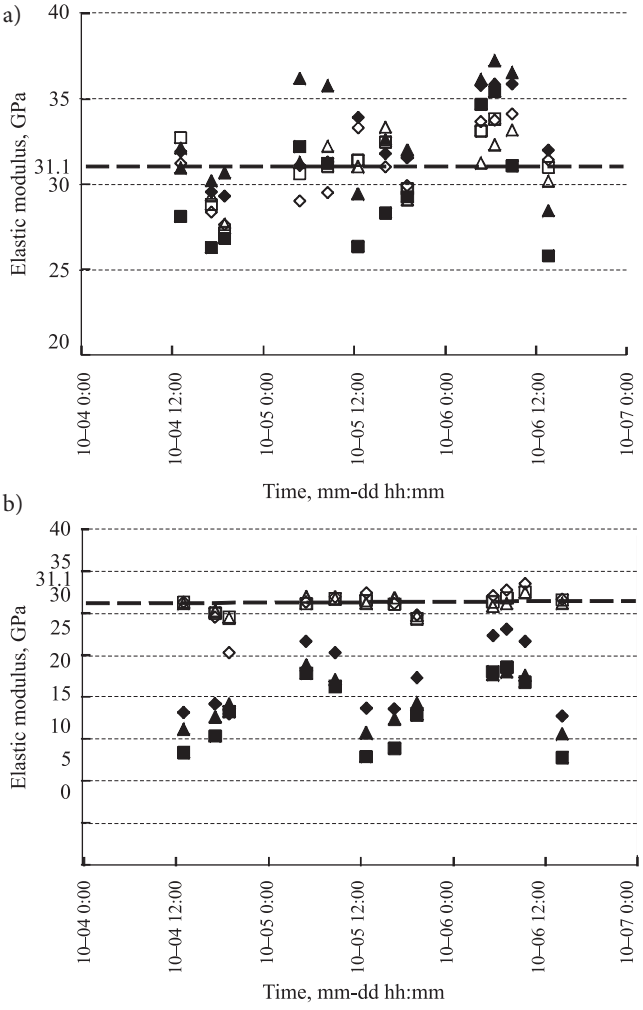

Fig. 9. Corrected elastic modulus: a – AREA method; b – MET: ◆ Section 4–0 backcalculated; ■ Section 5–0 backcalculated; ▲ Section 6–0 backcalculated; ◇ Section 4–0 corrected; □ Section 5–0 corrected; △ Section 6–0 corrected

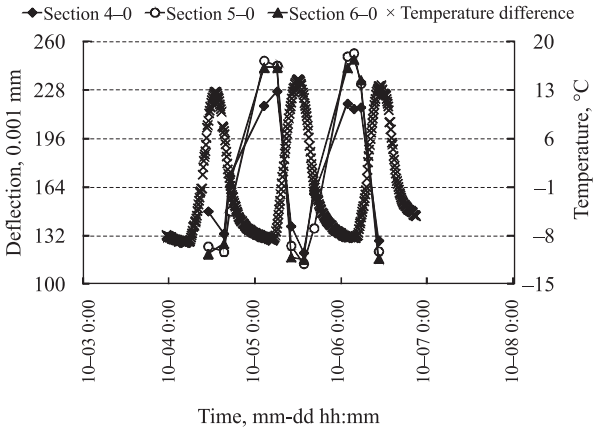

Fig. 10. Joint deflection measured at loading point

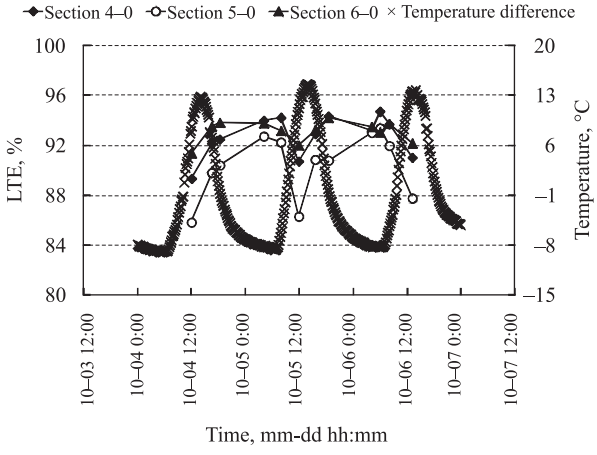

Fig. 11. LTE of joint

higher correlation of the former with the temperature difference. The extensively ranged elastic modulus approached the measured value by following the adjustment procedure. The effective built-in temperature difference composed of hourly temperature difference, built-in temperature difference, and irreversible shrinkage and creep may need to be used in Eq (6) in order to precisely adjust the backcalculated elastic modulus (Jeong, Zollinger 2005; Rao, Roesler 2005).

4. Curling effect on LTE of joints

The joint deflections of the concrete pavement sections were also measured under FWD loading. The joint loading positions were in the outer wheel path of the slabs. The trend of the joint deflections is opposite to that of the slab centres, because the vertical movements of the joints due to the curling were opposite to the movements of the slab centres. As shown in Fig. 10, the upward joint movement developed in the morning caused an increase in the joint deflection while the relative downward movement of the slab centre at the time caused a decrease in the deflection of the slab centre. On the contrary, joint deflection decreased in the afternoon, because of the downward curling. The decreased joint deflection in the afternoon suggested that the bottom of the transverse edge of the slab had more contact and consequently had to be supported by the subbase because of the downward slab curling. The joint deflections in sections 5-0 and 6-0 were slightly larger than those of section 4-0. The differences in the joint deflections increased in the morning due to the upward slab curling.

The LTE of the joints were calculated using the deflections of the loaded and unloaded adjacent transverse edges of the slabs as follows:

$$LTE = \frac{\delta_u}{\delta_l} 100, \tag{8}$$

where *LTE* –load transfer efficiency, %; δ_u – deflection of transverse slab edge where load is not applied; δ_l – deflection of transverse slab edge where load is applied.

The joints showed a max peak of LTE in the morning, as shown in Fig. 11, because dowel locking due to the upward slab curling increased the friction between the dowels and concrete slabs at the joints (Davids *et al.* 2003; Jeong 2008; Shoukry *et al.* 2004; William *et al.* 2001). The upward slab curling continuously increased during the slab's lifetime because of a greater amount of drying shrinkage at top of the concrete slab than at the bottom. The dowel locking caused by the long-term upward slab curling due to differential drying shrinkage further increased the LTE, particularly in the morning due to the negative temperature difference between the top and bottom of the slab. More specifically, the dowel locking restrained the free movement of both the loaded and unloaded transverse edges of the slab and, as a result, the LTE increased. The LTE of the slabs in sections 5–0 and 6–0 were larger than those of section 4–0.

5. Conclusions

The effect of the slab curling on the backcalculated structural capacity of the jointed concrete pavements was investigated using the deflection basins measured by a series of FWD tests. The measured deflections of the slabs showed almost the same trend as the ambient temperature and the temperature difference between the top and bottom of the concrete slab, which resulted in daily cycles. Larger deflections of the slab centres were measured in the afternoon, when the downward curling of the slab developed, due to the positive temperature difference while smaller deflections were recorded in the morning. The foundation moduli backculated by the deflection basins of the slabs were also significantly affected by the temperature difference. The foundation moduli increased in the morning and then decreased in the afternoon because of the slab curling. The elastic moduli of the pavement layers were backcalculated using the AREA method and MET. The backcalculated elastic modulus was also

significantly influenced by the slab curling, showing a similar trend to the deflection and foundation modulus of the concrete slab. A basic adjustment concept for the backcalculated elastic modulus using the temperature difference between top and bottom of the slab was suggested. The variations in the joint deflection and LTE verified the effect of the slab curling on the backcalculated structural capacity. Dowel locking due to the upward curling of the slab affected the LTE. Additional effort is needed in order to verify the effects of the built-in temperature and moisture warping on the backcalculated structural capacity of concrete pavements.

Acknowledge

The research in this paper was sponsored by the Expressway & Transportation Research Institute (ETRI) of the Korea Expressway Corporation (KEC) and a research project of "Development of Construction and Maintenance Technology for Low-Carbon Green Airport Pavements" funded by the Ministry of Land, Transport and Maritime Affairs (MLTM) and the Korea Institute of Construction & Transportation Technology Evaluation and Planning (KICTEP).

References

Davids, W. G.; Wang, Z.; Turkiyyah, G.; Mahoney, J. P.; Bush, D. 2003. Three-Dimensional Finite Element Analysis of Jointed Plain Concrete Pavement with EVERFE2.2, *Transportation Research Record* 1853: 92–99. http://dx.doi.org/10.3141/1853-11

Hall, K. T.; Mohseni, A. 1991. Backcalculation of Asphalt Concrete-Overlaid Portland Cement Concrete Pavement Layer Moduli, *Transportation Research Record* 1293: 112–123.

Hoffman, M. S.; Thompson, M. R. 1982. Backcalculating Nonlinear Resilient Moduli from Deflection Data, *Transportation Research Record* 852: 42–51.

Ioannides, A. M. 1990. Dimensional Analysis in NDT Rigid Pavement Evaluation, *Journal of Transportation Engineering* 116(1): 23–36. http://dx.doi.org/10.1061/(ASCE)0733-947X(1990)116:1(23)

Jeong, J. H. 2008. Environmental Effect on Development of Pavement Joint Cracks, in *Proc. of the ICE – Transport* 161(2): 55–63. http://dx.doi.org/10.3141/1947-07

Jeong, J. H.; Lee, J. H.; Suh, Y. C.; Zollinger, D. G. 2006. Effect of Slab Curling on Movement and Load Transfer Capacity of Saw-Cut Joints, *Transportation Research Record* 1947: 69–78. http://dx.doi.org/10.1061/(ASCE)0733-947X(2005)131:2(140)

Jeong, J. H.; Zollinger, D. G. 2005. Environmental Effects on the Behaviour of Jointed Plain Concrete Pavements, *Journal of Transportation Engineering* 131(2): 140–148. http://dx.doi.org/10.1016/S0963-8695(99)00034-1

Karadelis, J. N. 2008. A Numerical Model for the Computation of Concrete Pavement Moduli: a Non-Destructive Testing and Assessment Method, *NDT & E International* 33(2): 77–84.

Li, S.; White, T. D. 2000. Falling-Weight Deflectometer Sensor Location in the Backcalculation of Concrete Pavement Moduli, *Journal of Testing and Evaluation* 28(3): 166–175. http://dx.doi.org/10.1520/JTE12091J

Lin, P. S.; Wu, Y. T.; Juang, C. H.; Huang, T. K. 1998. Back-Calculation of Concrete Pavement Modulus Using Road-Rater Data, *Journal of Transportation Engineering* 124(2): 123–127. http://dx.doi.org/10.1061/(ASCE)0733-947X(1998)124:2(123)

Mohamed, A. R.; Hansen, W. 1997. Effect of Nonlinear Temperature Gradient on Curling Stress in Concrete Pavement, *Transportation Research Record* 1568: 65–71. http://dx.doi.org/10.3141/1568-08

Rao, S.; Roesler, J. R. 2005. Characterizing Effective Built-In Curling from Concrete Pavement Field Measurements, *Journal of Transportation Engineering* 131(4): 320–327. http://dx.doi.org/10.1061/(ASCE)0733-947X(2005)131:4(320)

Shoukry, S. N.; William, G. W.; Riad, M. Y. 2004. Validation of 3DFE Model of Jointed Concrete Pavement Response to Temperature Variations, *International Journal of Pavement Engineering* 5(3): 123–136. http://dx.doi.org/10.1080/10298430412331296525

Šiaudinis, G. 2006. Relationship of Road Pavement Deformation Moduli, Determined by Different Methods, *The Baltic Journal of Road and Bridge Engineering* 1(2): 77–81.

Talvik, O.; Aavik, A. 2009. Use of FWD Deflection Basin Parameters (Sci, Bdi, Bci) for Pavement Condition Assessment, *The Baltic Journal of Road and Bridge Engineering* 4(4): 196–202. http://dx.doi.org/10.3846/1822-427X.2009.4.196-202

Ullidtz, P. 1987. *Pavement Analysis*. Elsevier Science & Technology Books. ISBN: 0444428178

Westergaard, H. M.; Holl, D. L.; Bradbury, R. D.; Spangler, M. G.; Sutherland, E. C. 1939. Stresses in Concrete Runways of Airports, Highway Research Board 19: 197–202.

William, G. W.; Shoukry, S. N. 2001. 3D Finite Element Analysis of Temperature-Induced Stresses in Dowel Jointed Concrete Pavements, *ASCE International Journal of Geomechanics* 1(3): 291–308. http://dx.doi.org/10.1061/(ASCE)1532-3641(2001)1:3(291)

Received 13 September 2010; accepted 21 June 2011